Paleoceanography and Paleoclimatology

RESEARCH ARTICLE
10.1029/2017PA003297

Key Points:
- We present a new stable isotope and dust record from Taylor Glacier, Ross Sea area, Antarctica
- The Taylor Glacier record is incompatible with North-South synchronous deglacial warming
- TD2015: A revised Taylor Dome time scale for both ice and gas phases is introduced

Supporting Information:
- Supporting Information S1
- Data Set S1
- Data Set S2

Correspondence to:
D. Baggenstos,
baggenstos@climate.unibe.ch

Citation:
Baggenstos, D., Severinghaus, J. P., Mulvaney, R., McConnell, J. R., Sigl, M., Maselli, O., et al. (2018). A horizontal ice core from Taylor Glacier, its implications for Antarctic climate history, and an improved Taylor Dome ice core time scale. *Paleoceanography and Paleoclimatology*, *33*, 778–794. https://doi.org/10.1029/2017PA003297

Received 28 NOV 2017
Accepted 4 JUN 2018
Accepted article online 12 JUN 2018
Published online 19 JUL 2018

A Horizontal Ice Core From Taylor Glacier, Its Implications for Antarctic Climate History, and an Improved Taylor Dome Ice Core Time Scale

Daniel Baggenstos[1], Jeffrey P. Severinghaus[1], Robert Mulvaney[2], Joseph Robert McConnell[3], Michael Sigl[3], Olivia Maselli[3], Jean-Robert Petit[4], Benjamin Grente[4], and Eric J. Steig[5]

[1]Scripps Institution of Oceanography, UC San Diego, La Jolla, CA, USA, [2]British Antarctic Survey, Natural Environment Research Council, Cambridge, UK, [3]Department of Hydrologic Sciences, Desert Research Institute, Reno, NV, USA, [4]University Grenoble Alpes, CNRS, IRD, Grenoble INP, IGE, Grenoble, France, [5]Department of Earth and Space Sciences, University of Washington, Seattle, WA, USA

Abstract Ice core records from Antarctica show mostly synchronous temperature variations during the last deglacial transition, an indication that the climate of the entire continent reacted as one unit to the global changes. However, a record from the Taylor Dome ice core in the Ross Sea sector of East Antarctica has been suggested to show a rapid warming, similar in style and synchronous with the Oldest Dryas—Bølling warming in Greenland. Since publication of the Taylor Dome record, a number of lines of evidence have suggested that this interpretation is incorrect and reflects errors in the underlying time scale. The issues raised regarding the dating of Taylor Dome currently linger unresolved, and the original time scale remains the de facto chronology. We present new water isotope and chemistry data from nearby Taylor Glacier to resolve the confusion surrounding the Taylor Dome time scale. We find that the Taylor Glacier record is incompatible with the original interpretation of the Taylor Dome ice core, showing that the warming in the area was gradual and started at ~18 ka BP (before 1950) as seen in other East Antarctic ice cores. We build a consistent, up-to-date Taylor Dome chronology from 0 to 60 ka BP by combining new and old age markers based on synchronization to other ice core records. The most notable feature of the new TD2015 time scale is a gas age—ice age difference of up to 12,000 years during the Last Glacial Maximum, by far the largest ever observed.

1. Introduction

The transition from the last glacial period to the Holocene is of great interest because it is a time of large-scale changes to the climate system. The thermal bipolar seesaw model (Stocker & Johnsen, 2003) is able to explain most of the first-order variability. It postulates that the state of the Atlantic Meridional Overturning Circulation (AMOC) determines the hemispheric temperature contrast between the North and the South through heat flux changes in the Atlantic and the Southern Ocean. The bipolar seesaw is manifested in an Antarctic warming trend while Greenland is cold, and an Antarctic cooling trend while Greenland is warm (EPICA Community Members, 2006; WAIS Divide Project Members, 2015). Independent evidence from ocean circulation proxies (McManus et al., 2004) also emphasize the integral role of the AMOC during the deglaciation, with the period of Antarctic warming coinciding, within uncertainties, with AMOC reduction.

The response to these large-scale, abrupt changes in the climate system presents a challenge for numerical climate models. North Atlantic "hosing" experiments under glacial boundary conditions, where the AMOC is shut off by imposing large freshwater fluxes into the North Atlantic, have shown a range of changes in Antarctic climate as a result of the AMOC shutdown (Kageyama et al., 2013). While most models indicate a continent-wide coherent warming, some models (e.g., Timmermann et al., 2010) have produced changes of opposite signs in coastal areas, implying that regional climate dynamics can dominate the response, at least on centennial time scales. It is difficult to estimate the long-term response of these models because of the limited duration of most simulations. Buiron et al. (2012) also present a model that produces a dipole pattern (cooling in West Antarctica, warming in East Antarctica) in response to a 419-year-long forced AMOC shutdown under Last Glacial Maximum (LGM) boundary conditions. The mechanism responsible for this behavior appears to be

atmospheric teleconnections originating from the Tropics. However, in a synthesis of circum-Antarctic climate records from the last glacial period (Marine Isotope Stage 3), Buiron et al. (2012) cannot find such a dipole signal. As a benchmark not only for global climate models but also for conceptual models, it is crucial to know whether all of Antarctica went through the deglacial transition as a single unit.

Temperature proxy records from ice cores drilled throughout all of Antarctica agree to first order on a synchronous, spatially coherent deglacial warming signal (Pedro et al., 2011). There is also evidence for regional differences superimposed on the continent-wide trend, for example, a slower warming rate in the Atlantic sector from 16.0 to 14.5 ka BP (Stenni et al., 2011), or an earlier initial warming in West Antarctica compared to the East Antarctic records. The predominant pattern of warming from roughly 18 ka BP to Antarctic Isotope Maximum (AIM) 1, followed by a slight cooling during the Antarctic Cold Reversal (ACR) into another warming up to AIM 0, is common and synchronous to almost all ice core records from Antarctica. Identification of the AIM features in Antarctic isotope records is given in EPICA Community Members (2006). The isolation caused by the circumpolar upwelling of old deep water (Toggweiler & Samuels, 1995) and the difficulty of propagating oceanic temperature anomalies across the Antarctic Circumpolar Current (Armour et al., 2016) can explain why no abrupt climate changes are expected in Antarctica. The only record that appeared to not support this en bloc behavior is from the Taylor Dome ice core, where a more Greenland-like temperature evolution was hypothesized (Steig et al., 1998). This interpretation was subsequently challenged by Mulvaney et al. (2000) who questioned Steig et al. (1998)'s st9810 time scale because of poor agreement of the Taylor Dome decrease in calcium concentration during the deglaciation in comparison with other ice cores from East Antarctica. Dissolved calcium is (during the glacial) a proxy for particulate dust (Ruth et al., 2008), mostly of South American origin, the fine fraction of which is transported to Antarctica and deposited onto the ice sheet (Lunt & Valdes, 2001). Because the dust source is far removed from the deposition site, it is thought that changes in wind strength and precipitation in the source region, as well as changing washout by rain during the transport phase are the main factors influencing dust deposition in Antarctica (Fischer et al., 2007; Lambert et al., 2008). Thus local deposition effects are second order at most and changes in the dust flux are expected to be qualitatively similar in all Antarctic ice cores under glacial climate conditions (Schüpbach et al., 2013). In Grootes et al. (2001), the authors of the st9810 chronology acknowledge inconsistencies in the original time scale and tie the deep part of the record directly to Vostok δD variations. On this new time scale, the calcium decrease during the deglaciation is in agreement with other ice cores; however, by synchronizing δD, spatial homogeneity is assumed such that regional differences in climate are suppressed. Furthermore, the adjusted time scale is up to 7,000 years older than st9810, but the implications of this substantial modification are not explored.

It is instructive to step back and look at how st9810 was built. For every ice core, there are two separate time scales, one applying to the ice phase, and one to the gas phase, with the age difference of the two at a specific depth termed the gas age—ice age difference (Δage). This arises because air is able to mix relatively freely through the porous firn column and gets trapped in bubbles only at the bottom of the firn, where the ice is already hundreds to thousands of years old depending on site conditions (Schwander et al., 1988; Sowers et al., 1989). Ice age time scales in high accumulation sites are typically based on layer counting, but for most Antarctic ice cores (including Taylor Dome) this is not an option because the annual layers are too thin for accurate counting. The traditional workaround is to synchronize the gas time scale to a high accumulation rate core (commonly from Greenland) via globally well-mixed gases (Blunier et al., 2007) and estimate Δage using firn densification models. Δage for Greenland ice cores is on the order of hundreds of years, and its uncertainty does not contribute much to the total uncertainty in this procedure. Because of smaller accumulation rates, Δage in Antarctic ice cores is generally larger, commonly a few thousand years, and less well known (Bender et al., 2006). For Taylor Dome, Steig et al. (1998) used cosmogenic beryllium-10 concentrations (^{10}Be) as a proxy for accumulation rates (under the assumption of constant flux of ^{10}Be from the atmosphere to the ice; Steig et al., 1996), and δD for temperature, as inputs into the Herron-Langway densification model (Herron & Langway, 1980) to estimate Δage. The Grootes et al. (2001) correction to the initial time scale of up to 7,000 years, based on a comparison with other ice cores, suggests that the ice accumulation rate inferred from ^{10}Be was overestimated. Snow deposited on Taylor Dome may have blown away, to be deposited elsewhere (probably in the Dry Valleys), carrying with it the highly particle-reactive ^{10}Be and dust particles. This is supported by the analysis of Morse et al. (2007) who determined the accumulation history necessary to produce the Grootes et al. (2001) time scale. They conclude that accumulation-rate estimates from ^{10}Be and non-sea-salt sulfate overestimate the actual accumulation rate significantly during the LGM, possibly because

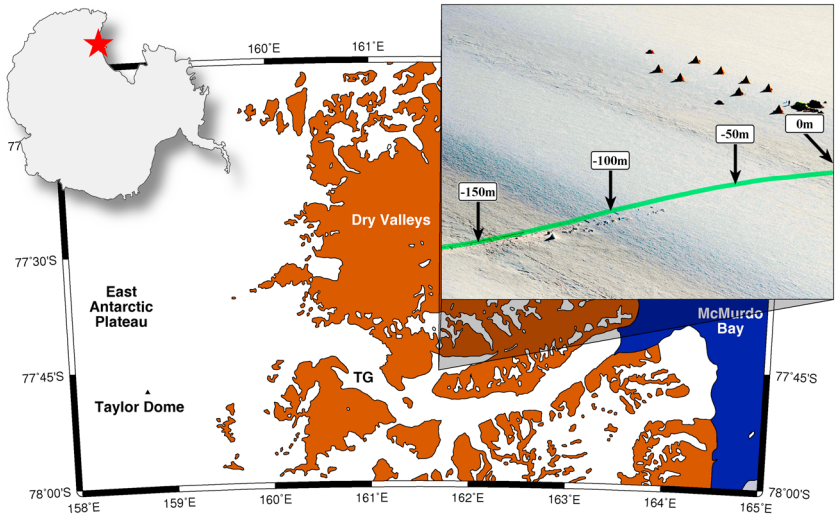

Figure 1. Map showing the location of the Taylor Glacier (TG) horizontal ice core in the southern McMurdo Dry Valleys, and Taylor Dome. Ice flowing into Taylor Valley originates on the northern flank of Taylor Dome, on the polar plateau. The aerial photo shows a close-up of the study site. In the lower left, the trench excavated for the horizontal ice core is visible. The trench cuts across a band of darker, slightly brown ice, representing the LGM and its high dust content. The green line represents the across-flow transect with markers indicating the distance scale used for sampling. Photo by J. Schwander.

of wind scour removing some of the initial snowfall. This somewhat confusing evolution of the Taylor Dome time scale has led many to believe that Taylor Dome is at best poorly dated (e.g., Jouzel et al., 2001; Morgan et al., 2002; Masson-Delmotte et al., 2011), yet it continues to be cited as an example of North-South synchronous climate change (e.g., Buiron et al., 2011; Davis et al., 2009; Farmer et al., 2005; Timmermann et al., 2010). For lack of availability of an updated, consistent chronology, the st9810 time scale is still the de facto Taylor Dome time scale (Aarons et al., 2016; Carlson & Clark, 2012; Schoenemann et al., 2014; Siddall et al., 2012). Recent results from another ice core drilled at nearby Talos Dome support the view that the climate evolution of the Ross Sea sector of Antarctica did not exhibit Greenland-like behavior (Stenni et al., 2011).

The aim of this paper is to revisit the puzzle of the Taylor Dome ice core and to present a new, up-to-date time scale. We use new data from the ablation zone of Taylor Glacier, a valley glacier formed by ice deposited on the northern slope of Taylor Dome (Figure 1), to confirm that the Taylor Dome deglacial temperature record is in phase with the rest of East Antarctica.

The concept of a horizontal ice core is based on the notion that ice buried in the accumulation zone surfaces again in the ablation zone (Reeh et al., 1991). If a continuous record can be identified, this marginal ice may be a valuable source for easily accessible large volume samples for paleoclimate studies (Aarons et al., 2017; Bauska et al., 2016; Petrenko et al., 2009). Ice from the northern flank of Taylor Dome descends eastward through the Transantarctic Mountains as Taylor Glacier and terminates in Taylor Valley (Kavanaugh & Cuffey, 2009). We therefore expect to find essentially the same ice that is buried beneath Taylor Dome to be exposed at the surface on Taylor Glacier. Possible complications include deformation of the ice, contamination because of the proximity to the surface, and finding too young/old ice if flow speeds are too fast/slow. An initial exploration of the Taylor Glacier ablation zone using stable water isotopes by Aciego et al. (2007) showed that vast quantities of glacial and deglacial transition ice are exposed over tens of kilometers. Recent work using atmospheric gases trapped in bubbles describes well-dated and continuous sections of ice covering the deglaciation and the LGM (Baggenstos et al., 2017). Here we present new glaciochemical, water-isotope and dust data from Taylor Glacier covering 49 to 16 ka BP. Section 2 describes the Taylor Glacier sampling and measurement setup in detail. The Taylor Glacier results, ice dating, and implications for continent-wide deglacial climate change are discussed in sections 3.1–3.4, while section 3.5 presents the new TD2015 time scale. A Δage and δ^{15}N modeling exercise to reconstruct past accumulation rates completes our analysis (section 3.6).

2. Sampling and Analytical Procedures

Our sampling approach is guided by the data presented in Baggenstos et al. (2017), which establishes transects and gas age models for Taylor Glacier. All samples used in this study are from a 120-m-long section on the across-flow transect that was dated using gases to the interval 47.7–14.6 ka BP. The stratigraphy on Taylor Glacier exhibits deformation features such as folding and irregular thinning typical of glacial ice. However, the sampling line presented here is continuous and not complicated by folding, as evidenced by the gas and glaciochemical records. The transect is oriented perpendicular to the flow direction, which is the preferred sampling orientation since layers of equal age (isochrones) lie parallel to the ice flow direction. The dip of the layers is approximately vertical, based on gas measurements and visual evidence from a 1.5-m-deep pit. We adopt the distance registration of the across-flow transect established by Baggenstos et al. (2017), where our sampling section covers −90 to −210 m on a distance scale whose zero point is tied to a conspicuous but arbitrary stratigraphic feature on the glacier surface (Figure 1). The primary measurements are continuous-flow analysis of non-sea-salt calcium (nssCa), $\delta^{18}O$ of ice, and insoluble particle mass over the full 120-m section. These data are supplemented by discrete measurements of insoluble dust mass and dust size distribution, as well as other continuous and discrete $\delta^{18}O_{ice}$ measurements performed in a different lab. Samples were collected in the 2010/2011, 2011/2012, and 2013/2014 field seasons. The ice surface is subhorizontal, with no crevasses, but thermal-contraction cracks are pervasive. Wind-blown dust gathers on surface irregularities and melts into the ice through radiative heating, forming cryoconite holes. The largest depth to which this surface contamination is observed is 40 cm. All our samples are from 70 to 100 cm depth to avoid surface contamination artifacts. Some thermal contraction cracks are filled with wind-blown snow, presumably as a result of wintertime katabatic storms that blow fresh snow from the polar plateau into the valleys. These wind-blown snow layers are up to 3 mm thick, and we estimate that they may contribute up to 1% of the total sample volume.

2.1. Continuous-Flow Analysis

For the continuous samples, a trench of 50 cm depth was excavated, and a clean (oil-free) electric chainsaw was used to cut ice sticks with dimensions of 50 cm × 5 cm × 5 cm from the entire length of the trench. The sampling depth for these samples is 70 to 80 cm. The ice sticks were later trimmed to 50 cm × 3.5 cm × 3.5 cm using a band saw in McMurdo. Major ion concentrations in the ice were measured at the Ultra Trace Chemistry Laboratory at the Desert Research Institute. The ice stick samples were melted continuously on a melter head that divides the melt water into three parallel streams. Elemental measurements were made on melt water from the innermost part of the core with ultrapure nitric acid added to the melt stream immediately after the melter head; potentially contaminated water from the outer part of the ice was discarded. Elemental analysis of the innermost melt water stream was performed in parallel on two inductively coupled plasma mass spectrometers (ICPMS, *Element2*), each measuring a different set of elements; some elements were analyzed on both.

The dual state-of-the-art ICPMS setup allows for measurement of a broad range of 30 elements described in detail elsewhere (McConnell et al., 2002, 2007, 2017). In particular, the measurement of calcium by ICPMS includes both soluble and insoluble fractions, whereas the traditional measurement technique by ion chromatography only registers the soluble fraction. The continuous-flow system also includes a cavity ring-down water isotope analyser (L2130-i, Picarro Inc.) that measures stable isotope ratios (i.e., $\delta^{18}O$) of the melt water (Maselli et al., 2013). The effective resolution of this sampling setup is approximately 1 cm. The insoluble particle count data were measured with an Abakus laser particle counter with an effective measurement size range of ∼0.8 to 10 μm (Ruth et al., 2008). Both the Abakus and the Coulter counter measurements (described below) are based on particle volume, and a particle density has to be assumed for the conversion to mass. This assumed density is 2.5 g/cm^3 for both instruments.

2.2. Discrete Samples for Dust Analysis

The same transect was discretely sampled with a PICO ice coring drill (3-in. diameter; Koci & Kuivinen, 1984) for measurements of insoluble dust. For each sample, a 1-m-deep core was recovered and a cylinder of 2 cm height was cut from the bottom of the core with a clean hand saw. The sampling spacing is 30 cm from −90 to −140 m, and 1 m from −140 to −180 m. These samples were sent frozen to the Laboratoire de Glaciologie et Géophysique de l'Environnement (LGGE), now Institut des Géosciences de l'Environnement (IGE) in Grenoble, France, for analysis of dust mass and dust size distribution. The ice samples were decontaminated by repeat

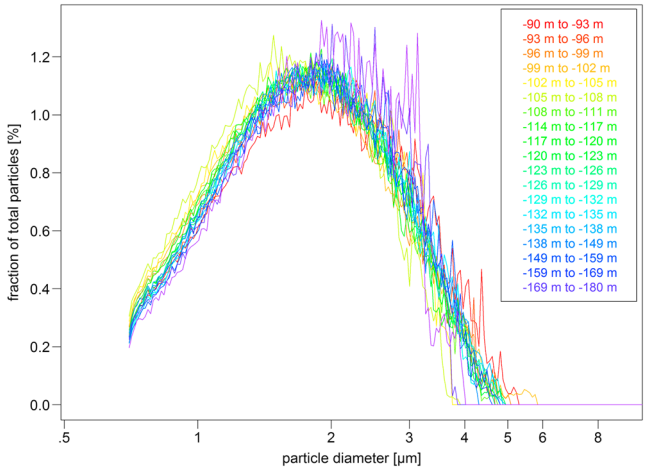

Figure 2. Average dust size distributions from different sections of the transect. Colors denote sections of increasing age, from youngest (red) to oldest (purple). There is no indication of any local dust sources. Measurements made by Benjamin Grente and Jean-Robert Petit at the Laboratoire de Glaciologie et Geophysique de l'Environnement, Grenoble by Coulter counter.

washings in ultrapure water. The measurements were performed using a Multisizer IIe(c) Coulter counter setup in a class 100 clean room. Detailed decontamination and measurement procedures are described by Delmonte et al. (2002).

2.3. Additional Measurements of $\delta^{18}O_{ice}$

We subsampled both the continuous ice sticks and the discrete cylindrical ice samples for stable water isotope analysis. Twenty-five-centimeter-long slabs of 2- to 3-mm thickness were shaved off of one side of the continuous samples from −90 to −170 m. The same procedure was applied to all discrete samples. These slabs of ice were later melted in Ziploc bags, and the meltwater was transferred into 30-ml wide mouth HDPE sampling bottles, and sent for analysis to the Institute of Arctic and Alpine Research (INSTAAR). Measurements were performed using a CO_2 equilibration system (Epstein & Mayeda, 1953) coupled to a Micromass SIRA Series II Dual Inlet mass spectrometer following well-established procedures. The stated 1-sigma precision of the INSTAAR $\delta^{18}O$ measurements is 0.036‰.

3. Results and Discussion

3.1. Quality of the Dust Record

Patagonia has been identified as the major source of dust in Antarctic ice cores during the last glacial period (Basile et al., 1997; Delmonte et al., 2017; Grousset et al., 1992) and changes in the dust flux are attributed to aridity and wind strength in the source and transport path regions (Lunt & Valdes, 2001). The first-order dust signal throughout Antarctica is quite uniform, despite large differences in dust concentrations due to widely varying accumulation rates and dust deposition fluxes. For the Taylor Glacier dust record to be useful as a dating tool, we must show that (a) it has not been compromised by additional local dust sources either during deposition on the polar plateau or at our sampling site via cracks or cryoconites, and (b) that the dust signal is qualitatively similar to records from deep ice cores. Figure 2 shows the dust size distribution of 164 samples averaged in 20 bins. All parts of the record have a unimodal, close to lognormal distribution with a maximum at ~2 µm and very few particles larger than 5 µm. This size distribution is characteristic of long-range dust transport and consistent with observations from, for example, Dome C (Delmonte et al., 2004), EDML (Wegner, 2008), and Talos Dome (Delmonte et al., 2010), all of which show the same mode around 2 µm in the glacial period. For the Holocene, some studies (e.g., Albani et al., 2012, in the Talos Dome ice core) have found significant contributions from local sources. The fact that there are few particles larger than 5 µm in the Taylor Glacier record strongly suggests that the contribution of local dust sources to the total measured dust load in our samples is insignificant. Aarons et al. (2017) also measured dust size distributions as well as concentrations on samples from the same sampling transect on Taylor Glacier, but from a depth of 6 to 7 m where surface contamination can safely be ruled out since no cracks are observed to penetrate to that depth. During the glacial period, they find few particles larger than 5 µm, the total mass of which is at least an order of magnitude smaller than the mass of the fine particle fraction. The dust concentration record is thus not measurably biased by addition of locally sourced material in the deposition area. The implications of the changes in the dust size distribution with time with regards to atmospheric transport history are discussed in detail by Aarons et al. (2017).

The raw dust and nssCa records (Figure 3) are highly correlated, as expected since the soluble dust fraction is mostly composed of nssCa. Insoluble dust mass measured with different techniques on discrete ice samples and continuous ice samples agree well with each other on the main features, but a more detailed comparison is hampered by high levels of noise. The dust mass data from the discrete samples are consistently higher by approximately 0.1 ppb than the data from the continuous flow. This discrepancy may be explained by differences in the measurement techniques, for example, in the continuous-flow analysis system, the meltwater stream is forced through a 10-µm filter, which may also capture a nonnegligible fraction of particles smaller than 10 µm. Furthermore, the Coulter counter captures a slightly larger range of particle sizes (0.7 to 20.0 µm) than the Abakus. Another aspect to consider is that ice core dust is generally nonspherical, which affects the Abakus and Coulter counter in different ways (Simonsen et al., 2018). The insoluble dust mass data from Aarons from Aarons et al. (2017; also determined by Coulter counter) are similarly elevated with respect to the Abakus data, supporting the idea that the discrepancy is due to measurement techniques.

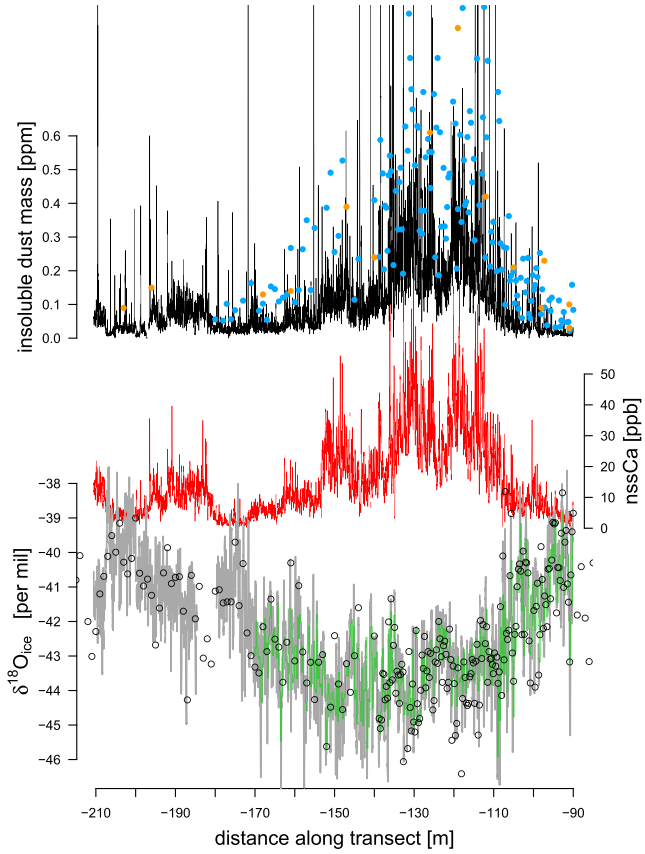

Figure 3. Raw data for insoluble dust mass (top), nssCa (center), and $\delta^{18}O_{ice}$ (bottom) from the Taylor Glacier horizontal ice core. Data from high-resolution continuous-flow analysis is shown in black (top), red (center), and gray (bottom). Discrete samples for insoluble dust concentration are shown as blue (this study) and orange circles (Aarons et al., 2017). $\delta^{18}O_{ice}$ 25-cm averages (green line) and discrete samples (black circles) measured at the Institute of Arctic and Alpine Research (INSTAAR) are in excellent agreement with the continuous-flow data.

Nonetheless, the good agreement of insoluble dust mass and nssCa concentrations (correlation coefficient $r = 0.76$ for 10-cm averages) gives us confidence to use nssCa as a proxy for long range dust loading. From here on, we will use only nssCa as a dust proxy to compare with other deep ice core records because Taylor Dome has a nssCa record but no high-resolution insoluble dust data.

The elevated values for nssCa concentration from −110 to −150 m in the transect are indicative of the LGM. The shape of the dust record compares favorably with Antarctic deep ice cores, all of which have three distinctive maxima in dust concentration during the LGM, separated by periods of relatively warm climate and reduced dust deposition known as Antarctic Isotope Maximum (AIM) 2 and 4. Assuming no hiatuses in the record, which is well justified given the good agreement of the nssCa record with traditional deep ice cores (Figure 4), the sections with very low dust loading from −170 to −180 m and −195 to −205 m should then correspond to AIM 8 and 12, respectively.

3.2. Dating Taylor Glacier

A gas age time scale for Taylor Glacier was developed by Baggenstos et al. (2017) based on synchronization of gas proxies to the WAIS Divide ice core. The ice age time scale is developed here. Because the thinning and thus the accumulation rate history of the Taylor Glacier ice is poorly known, it is ineffective to apply firn densification models to estimate Δage in order to derive the ice age time scale. To create the ice age time scale, we make the assumption that dust transport to Antarctica is the main factor in determining local dust deposition fluxes, causing reconstructed dust records from different locations to all look identical to first order. This allows us to date our transect by synchronizing changes in nssCa concentration to equivalent changes in the WAIS Divide ice core (supporting information Table S1 and Figure 4). We chose the WAIS Divide ice core as our reference record because of its demonstrated high dating accuracy and its high-resolution nssCa

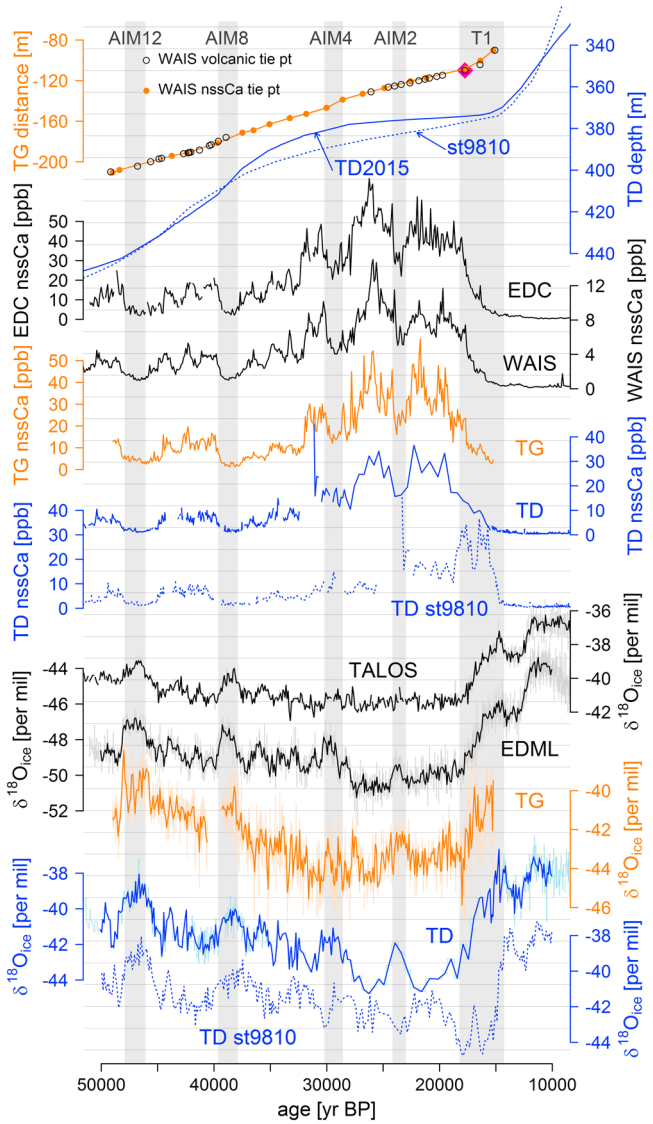

Figure 4. Ice chemistry records on a common time scale. From top to bottom: Taylor Glacier distance-age curve (orange) synchronized to the WD2014 time scale using nssCa tie points (orange) and volcanic events (black); Taylor Dome depth-age curve for the new TD2015 time scale (blue, solid) and Steig et al. (1998)'s st9810 time scale (blue, dotted); EPICA Dome C nssCa (black, Fischer et al., 2007; Wolff et al., 2006), WAIS Divide nssCa (black, Sigl et al., 2016), Taylor Glacier nssCa (orange), Taylor Dome nssCa on TD2015 time scale (blue, solid), and on st9810 (blue, dotted); stable water isotopes for TALDICE (black, Stenni et al., 2011), EPICA Dronning Maud Land (black, EPICA Community Members, 2006), Taylor Glacier (orange), and Taylor Dome (blue) on TD2015 (solid) as well as on st9810 (dotted) for comparison. All nssCa and water isotope records were binned into 100-year averages. For the isotope records, the faint colored lines represent the raw data while the bold lines show the binned averages. The pink square highlights the 17.7 ka Mt Takahe volcanic event.

data (Buizert et al., 2015; WAIS Divide Project Members, 2013; Sigl et al., 2016). In between the tie points we apply a linear interpolation. Fudge et al. (2014) show that more complex interpolation schemes taking into account annual layer thicknesses or accumulation rates produce more accurate age models, but since we do not have good constraints on either annual layer thickness or accumulation rate, we resort to the use of the traditional, linear method. The difference between the interpolation schemes should be small to negligible if a large number of tie points can be identified. In addition to the tie points from the nssCa synchronization, we were able to identify a number of volcanic events that are found in both our record and in the WAIS Divide ice core, based on distinct sulfur and cadmium anomalies (Table S2). This volcanic synchronization confirms and strengthens our time scale. Furthermore, the unique chemical fingerprint of the 17.7 k Mt. Takahe eruption (McConnell et al., 2017) is clearly identified in the record, allowing us to securely constrain the beginning of

the deglaciation. The resulting distance-age relationship is close to linear from 49 to 17 ka BP, with a hint of a steepening and thus possibly higher accumulation rates from 17 to 16 ka BP. A comparison with the gas age time scale shows that the ice age is slightly older than the gas age for the entire transect (Figure 7), as expected from firn densification. This lends additional support to our dating, since the gas and ice ages were determined independently from each other. The inferred average annual layer thickness, calculated as horizontal distance divided by time without correcting for thinning, is 0.35 cm/year.

3.3. $\delta^{18}O_{ice}$

Stable oxygen and hydrogen isotopes of H_2O in the ice are commonly used to infer past surface temperatures at the ice core deposition site (Jouzel et al., 1997). Figure 3 shows $\delta^{18}O_{ice}$ measured on discrete and continuous samples from the Taylor Glacier transect. The three records (DRI continuous, INSTAAR continuous, and INSTAAR discrete) agree very well with each other; after downsampling DRI continuous to the lower resolution record, $r = 0.97$ for DRI versus INSTAAR continuous and $r = 0.82$ for DRI versus INSTAAR discrete. The absolute values at certain obvious features are identical to the $\delta^{18}O_{ice}$ values measured in the Taylor Dome ice core (Figure 4; Steig et al., 1998): −39‰ during AIM 12, −40.5‰ during AIM 8, and −44‰ during the LGM. This close correspondence in the absolute values is a strong indication that the deposition site for Taylor Glacier is at approximately the same elevation as the Taylor Dome ice core. It also means that small amounts of snow blown into wintertime cracks and observed in our samples do not significantly alter the large scale nature of our record. However, the Taylor Glacier $\delta^{18}O_{ice}$ record is considerably noisier than $\delta^{18}O_{ice}$ records from other ice cores, even when 25-cm averages are considered. One reason for this could be the small amounts of modern snow in our samples; however, modern snow in the area is less depleted in the heavy isotopologue (Gooseff et al., 2006) and we would expect outliers only on the positive side, which is not what we observe. Another possibility is that the Taylor Glacier deposition site experiences more decadal variability than other ice cores precisely because the accumulation rate is very low. In such an arid regime, single snowfall events contribute a larger fraction of the total snow accumulation, which could explain the increased variability. A third factor to consider is that postdepositional processes can modify $\delta^{18}O$ values by several ‰ in low accumulation settings, as shown with modern measurements for a site at Taylor Mouth (a wind-scoured area near Taylor Dome; Neumann et al., 2005) and at Dome Fuji (Hoshina et al., 2014). Ventilation can redistribute and remove water vapor in the firn, which causes modification of isotope ratios through sublimation and condensation (Waddington et al., 2002). The lower the accumulation rate, the longer the firn remains near the surface, where it can be modified by ventilation. On the other hand, even if diffusion causes a significant change in the $\delta^{18}O$ values, one would expect that such a redistribution through vapor would smooth out the differences in $\delta^{18}O$ between different layers of ice.

Despite the overall good agreement between the Taylor Glacier and Taylor Dome $\delta^{18}O_{ice}$ records, there are clear differences: The signature of AIM events in Marine Isotope Stage 3 (~30 to 60 ka), which are evident in the EDML and Taylor Dome records, are much less pronounced in our new record. The elevated level of noise may be masking some of the features. Still, there appears to be less millennial-scale variability in the Taylor Glacier record. At 27 ka, when the EDML and Taylor Dome $\delta^{18}O_{ice}$ shifts to more depleted values, reflecting the coldest stages of the last glacial period, there is no change in the Taylor Glacier $\delta^{18}O_{ice}$. This absence of a clear glacial maximum is also observed in the Talos Dome ice core. The magnitude of the AIM 2 peak is slightly smaller at Taylor Glacier than at Taylor Dome, but it is larger than at EDML (EPICA Community Members, 2006) and Talos, and comparable to WAIS Divide (WAIS Divide Project Members, 2013). It is not the aim of this paper to examine what causes the differences in the $\delta^{18}O_{ice}$ records, but it is important to note that the main first-order features of variability in Antarctic climate history are imprinted in the Taylor Glacier record just as in other ice core records.

3.4. Asynchronous Climate Change at Taylor Dome and the North Atlantic

At Taylor Glacier, $\delta^{18}O_{ice}$ starts to increase significantly at approximately 18 ka BP (Figure 4). The timing of this increase is well constrained via the 17.7 k volcanic event (McConnell et al., 2017, Table S2). $\delta^{18}O$ of ice is typically interpreted as a proxy for the local condensation temperature, but changes in the atmospheric circulation and accumulation rate can also affect the isotopic composition of precipitation (Dansgaard, 1964). Naturally, changes in temperature, atmospheric circulation and accumulation rate are often convolved, complicating the interpretation of any $\delta^{18}O_{ice}$ record. For our purposes, it is sufficient to recognize that any one of these factors, and probably all of them, are changing starting at 18 ka BP, and that this change must be recorded in the Taylor Dome ice core as well because of the proximity of the deposition sites for Taylor Dome and Glacier. This observation directly contradicts the st9810 time scale, which showed no significant change

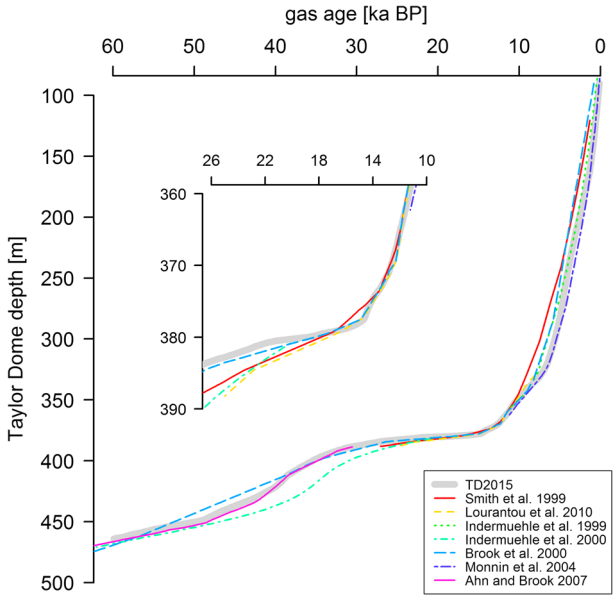

Figure 5. Existing Taylor Dome gas time scales and TD2015 from 0 to 60 ka BP. Insert shows close-up of the late Last Glacial Maximum (LGM) and the deglacial transition. There are large differences between individual time scales, especially from 35 to 55 ka BP, but also during the Holocene. During the deglacial transition the agreement between time scales is good, thanks to large and sometimes abrupt changes in all gases.

in $\delta^{18}O_{ice}$ until 15 ka BP. Furthermore, as pointed out by Mulvaney et al. (2000), the calcium records are also incompatible (Figure 4). Previously, one could have argued that Taylor Dome was indeed affected by different air masses and maybe should not have the same dust history as Dome C, especially if there was some sort of direct North-South Atlantic connection that determined climate in the western Ross Sea sector. But the new Taylor Glacier nssCa record is indisputably inconsistent with the st9810 chronology, demonstrating that the dust flux history in the Taylor Dome area was not significantly different from the rest of Antarctica. Our new findings confirm that the isotope warming at the start of the deglaciation in the Taylor Dome area begins at approximately 18 ka BP, just as in other East Antarctic ice cores.

3.5. TD2015—A New Time Scale for Taylor Dome

Although the validity of the original Taylor Dome ice time scale has been questioned previously, no updated time scale has yet been created for the deglaciation and the LGM. The additional, unambiguous evidence from Taylor Glacier presented here provides motivation to revisit this issue and produce a new Taylor Dome time scale based on all available information. We start with the Taylor Dome gas age, for which a number of different time scales have been published, with most of them only covering a certain part of the core (Figure 5): The Holocene (Indermühle et al., 1999) and deglaciation (Smith et al., 1999) CO_2 isotope studies both use the st9810 gas time scale, which is based on CH_4 and $\delta^{18}O_{atm}$ synchronization to the Greenland Ice Sheet Project 2 (GISP2) ice core. Brook et al. (2000) also use methane and $\delta^{18}O_{atm}$ measured in Taylor Dome to synchronize to GISP2, but the resulting time scale is significantly different from st9810, especially during the Holocene. Indermühle et al. (2000) present a CO_2 record from the last glacial period that is on a time scale built by matching CO_2 and CH_4 to the Vostok GT4 time scale. Monnin et al. (2004) matches the Holocene CO_2 record from Indermühle et al. (1999) to the Dome C CO_2 record. Using new and existing CO_2 and CH_4 data from 65 to 35 ka BP, Ahn and Brook (2007) also produced a new gas chronology for Taylor Dome, synchronized to GISP2. Finally, Lourantou et al. (2010) synchronize the deglacial CO_2 record from Smith et al. (1999) to the GICC05 time scale (Andersen et al., 2006; Rasmussen et al., 2006). The new TD2015 gas age was constructed via synchronization of the Taylor Dome $\delta^{18}O_{atm}$ signal together with fixed CO_2 and CH_4 tie points (supplementary information) to the equivalent record from the WAIS Divide ice core using the "match" algorithm developed by Lisiecki and Lisiecki (2002).

Unlike for the gas age, there have only been two new publicly available time scales published for the Taylor Dome ice age since the original st9810: Monnin et al. (2004) for the Holocene and more recently Sigl et al. (2014) for the last two millennia. We adopt the volcanic tie points of Sigl et al. (2014) from 0 to 153 m depth (equivalent to present to ~100 AD), which are based on matching volcanic sulfate peaks to the equivalent sulfur peaks in the WAIS Divide record. From 153 to 360 m depth, the ice age is estimated by adding the Monnin et al. (2004) Δage to the gas age at each depth. This procedure creates an inconsistency in the sense that Δage depends on the accumulation rate, which itself is a derivative of the time scale. Changing the time scale should thus also change Δage. However, the uncertainties in the modeling of Δage by Monnin et al. (2004) are expected to be larger than the change due to a small adjustment of the time scale, which is why we think this approach is justified. Before 16 ka BP, there are no features in the calcium record that could constrain the dating. We therefore make the assumption of a uniform ACR onset and end: We add two tie points at the beginning and the end of the ACR identified in the $\delta^{18}O_{ice}$ record (depths and ages in supplementary information), assuming that these large scale isotope changes are synchronous in all Antarctic ice cores as suggested by Pedro et al. (2011) and Stenni et al. (2011). In general, the dating in the mid to early Holocene as well as the late deglaciation is not as well constrained as in the periods where volcanic or calcium ties are available.

For the early deglaciation and glacial period, we synchronize the Taylor Dome calcium record to our Taylor Glacier nssCa record. To facilitate the synchronization, we convert Taylor Dome calcium and sodium concentrations to nssCa as described in Bigler et al. (2006). Using continuous-flow high-resolution measurements

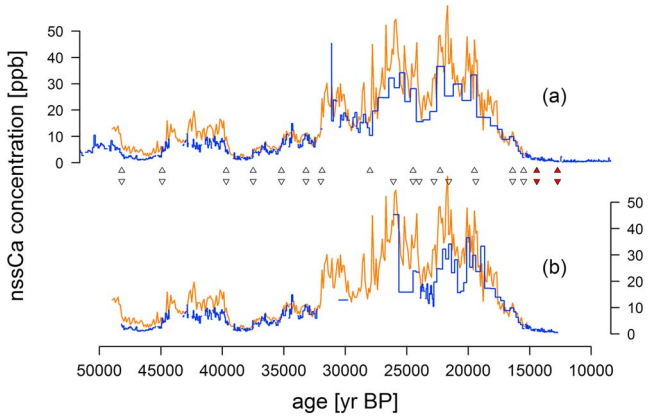

Figure 6. Synchronization of the Taylor Glacier (orange) and Taylor Dome (blue, Steig et al., 2000) nssCa records. Low sampling resolution and missing data complicate the synchronization. Shown are two options (a) and (b) along with the nssCa tie points used for both scenarios. Red triangles indicate the two additional tie points based on $\delta^{18}O_{ice}$.

from Dome C, they also determined the sodium/calcium ratios in sea salt and in crustal derived aerosols, which are necessary for the calculation of nssCa. We adopt their estimates, assuming that the crustal and sea salt sources are similar for aerosols deposited at Dome C and Taylor Dome. The correction to Ca is small, less than 2 ppb excluding the LGM, and less than 5 ppb during the dustiest intervals. The nssCa concentration at Taylor Glacier and Taylor Dome are very similar, with slightly higher values for Taylor Glacier. This is somewhat surprising since in continental Antarctica dust deposition is thought to occur mainly through dry deposition (Mahowald et al., 1999) which should lead to lower nssCa concentrations at Taylor Glacier because of its higher accumulation rate (still low accumulation overall). However, it is difficult to compare the nssCa concentrations directly, since the Taylor Glacier data was measured using ICPMS, which is able to quantify the soluble and insoluble calcium components, whereas the Taylor Dome data only consists of the soluble part.

A precise synchronization is complicated by two factors: The time resolution of the Taylor Dome chemistry record is only approximately one measurement every few hundred years during the LGM, because of the very low accumulation rate and a sample spacing/averaging of 0.2 m. In addition, there are no data available from a crucial part of the record, from 382.48 to 383.5 m depth and from 383.7 to 384.5 m depth. Taking this into account, there are two viable ways to synchronize the two records (Figure 6): Option (a) requires the accumulation rate to gradually decrease heading into the LGM, reaching a minimum at 25 to 20 ka BP, and then increase substantially into the early Holocene. For option (b) to work, accumulation has to fall sharply to extremely low levels at 32 ka BP, probably with significant hiatuses on the order of a few thousand years, before recovering gradually starting at 25 ka BP. This option has the advantage that the highest nssCa value measured in Taylor Dome matches the largest peak in Taylor Glacier, which is not the case for option (a). There are several lines of evidence that make a strong case for option (a): (1) Higher $\delta^{15}N$ at 30 ka than at 25 ka (Figure 8) suggests a thicker firn with higher accumulation rates at 30 ka, consistent with option (a). (2) $\delta^{18}O_{atm}$ does not show any irregularities but follows the atmospheric reference from 30 to 25 ka. If there were a hiatus of several millennia, the densification process would slowly come to a halt. If this had happened we should see a jump in $\delta^{18}O_{atm}$, not the continuous change that we observe. (3) The chemistry data of the soluble ions Na, Cl, K, and Mg do not have their maximum at the calcium spike, which suggests that a period of very low accumulation did not cause the calcium spike. (4) Independent estimates using ^{10}Be (Steig et al., 2000) and SO_4 (Morse et al., 2007) agree that the lowest accumulation rate was reached around 20 ka BP, with higher values around 30 ka BP. Overall, we find that option (a) is better supported by the available evidence, but is it difficult to completely rule out option (b).

Finally, for the period not covered by our Taylor Glacier record, that is 49 to 60 ka BP, we apply the same manual calcium matching procedure with WAIS Divide as the reference record. All used tie points were updated to the WD2014 reference. It is noteworthy that the new Taylor Dome TD2015 time scale is not only significantly different from st9810 during the glacial period; also in the Holocene the disparity amounts to up to 1,500 years.

The resulting depth-age curves for the gas and ice phase (Figure 7) are almost flat in the LGM because of the very low accumulation rate. A period of 8,000 years, from 24.5 to 16.5 ka BP, is compressed into 2.8 m depth. Our best estimate of the maximum Δage is ~12,000 years (at 378.5 m depth), significantly larger than the next-largest value of any ice core of 6,500 years that was estimated for the Vostok in the LGM (Veres et al., 2013). Our estimate is robust owing to good age constraints on both the gas and ice phase: At 378.5 m, CO_2 is already 220 ppm, methane is 450 ppb and rising, and $\delta^{18}O_{atm}$ is >1‰, which excludes any ages older than 15.5 ka BP. At the same depth, nssCa is 15 to 20 ppb, but elevated nssCa values between AIM 4 and AIM 2 preclude ages younger than 27 ka BP for the ice phase.

The Taylor Dome $\delta^{18}O_{ice}$ record, on the TD2015 time scale, looks qualitatively similar to isotope records from other Antarctic ice cores. AIM 2 features prominently during the LGM. Because of the exceptionally low accumulation rate, the time resolution of the isotope record is reduced, making precise comparisons difficult. Furthermore, because of the long residence time of the firn near the surface, it is possible that ventilation affected the isotope record considerably. Following AIM 2 there is a gradual but weak (isotope) warming

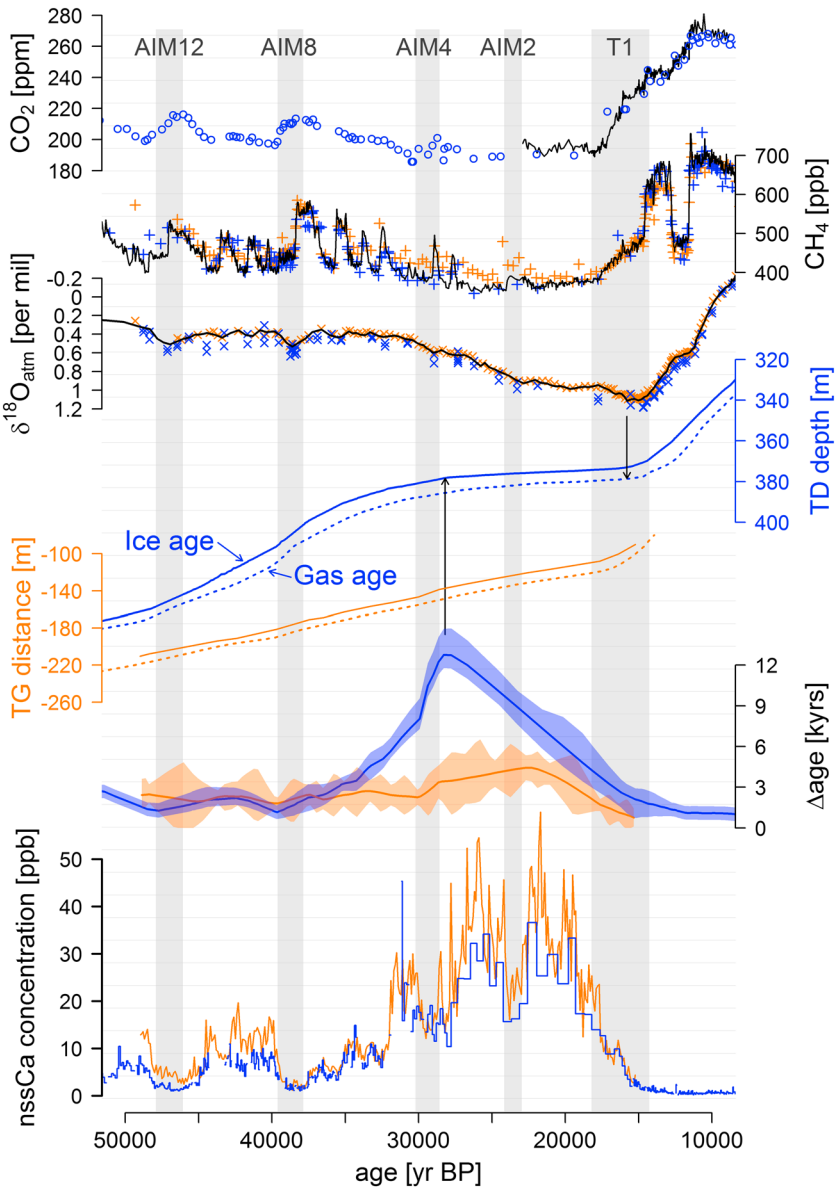

Figure 7. Δage, gas, and ice phase records for Taylor Glacier and Taylor Dome. From top to bottom: CO_2 concentration from Taylor Dome (blue, Ahn & Brook, 2007; Smith et al., 1999) and WAIS Divide (black, Marcott et al., 2014); CH_4 concentration from Taylor Dome (blue, Brook et al., 2000), Taylor Glacier (orange), and WAIS Divide (black, Buizert et al., 2015; WAIS Divide Project Members, 2013); $\delta^{18}O_{atm}$ from Taylor Dome (blue, Sucher, 1997), Taylor Glacier (orange), and WAIS Divide (black, Seltzer et al., 2017); Taylor Dome ice age (blue solid) and gas age (blue dotted) curves; Taylor Glacier ice age (orange solid) and gas age (orange dotted) curves; Δage for Taylor Dome (blue) and Taylor Glacier (orange) including an estimate of the uncertainty; nssCa from Taylor Dome (blue) and Taylor Glacier (orange). Taylor Dome records are on the TD2015 time scale. Δage is plotted on the ice age time scale. Black arrows point to 378.5 m depth for the gas and ice age. At 378.5 m, the Δage is approximately 12,000 years. Major AIM events and the beginning of the deglacial transition are highlighted in gray bars.

until 18 ka BP (similar to WAIS Divide), after which the warming rate increases substantially, in sync with the strong warming in all Antarctic records. As already discussed in Steig et al. (2000), Taylor Dome is unusual in that almost all of the deglacial isotope warming is accomplished by 14.7 ka BP, during the first half of the deglaciation. On this particular point we see no disagreement with the original interpretation.

3.6. $\delta^{15}N$ Modeling

There are no modern or past analogues for a firn column that takes 12,000 years for fresh snowfall to turn into ice, as required by our interpretation. The relevant physics may be substantially different from the physics

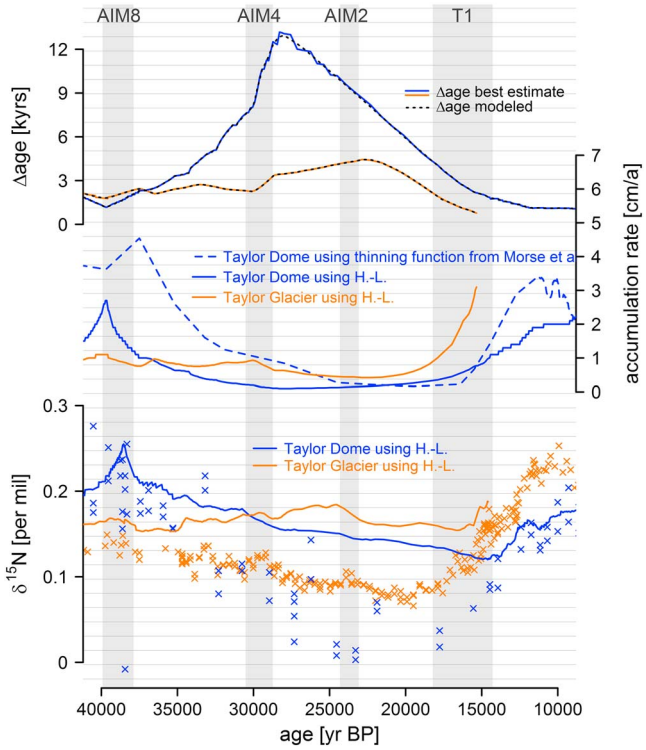

Figure 8. Δage modeling for Taylor Glacier and Taylor Dome and a comparison with δ^{15}N. For both Taylor Glacier and Taylor Dome, shown are modeled Δage (top), accumulation rate (center), and δ^{15}N (bottom), along with measurements of δ^{15}N (Baggenstos et al., 2017; Sucher, 1997). For Taylor Dome, a second accumulation rate history (dashed) was reconstructed by unthinning the TD2015 time scale using the thinning function from Morse et al. (2007). Major AIM events and the beginning of the deglacial transition are shown in gray bars.

implicit in firn densification models, which are built and calibrated for present day conditions. For example, physical processes such as vapor transport may dominate over mechanical deformation as densification mechanisms under low driving stress on these long time scales. However, as an exercise to illuminate the possible model limitations, we model Δage using an empirical steady-state firn densification model (Herron & Langway, 1980) together with δ^{15}N measurements (Baggenstos et al., 2017) to gain insight into the firn column during that unusual time. We chose the Herron-Langway model instead of other, more recent modeling approaches (e.g., Goujon et al., 2003) because it seems to have a more realistic sensitivity to accumulation variability (Buizert et al., 2015) and because of its simplicity. A site with 12,000 years Δage and <0.1 cm/year water equivalent accumulation is well outside of the calibration range of any firn densification model (Landais et al., 2006), so the results should be taken with a healthy dose of skepticism. The Herron-Langway model uses inputs of firn temperature and accumulation rate to predict density-depth profiles and thus indirectly firn thickness. Δage is approximated as the age of the ice at bubble close-off depth (close-off density parameterized as in Schwander et al., 1997), and the age of the gas at this depth is assumed negligible (on the order of a few decades). Firn thickness and accumulation rate then directly determine Δage. We run the Herron-Langway model in reverse, trying to find the accumulation rate that produces our observed Δage given a prescribed temperature. The temperature input is averaged over the measured Δage, representing an average temperature during the densification process. We convert the Taylor Dome isotope record into local temperature using $\alpha = 0.5$ ‰ $(°C)^{-1}$ as in Steig et al. (2000). We use the same approach to model Δage for Taylor Glacier. However, we use the Taylor Dome temperature instead of the Taylor Glacier temperature because of gaps in the Taylor Glacier record and unresolved doubts about whether the Taylor Glacier isotope record is a good proxy for local temperature (see section 3.3 for details).

The firn thickness can then be used to predict δ^{15}N assuming that gravitational settling is the only process affecting δ^{15}N in the firn (Craig et al., 1988; Sowers et al., 1989). The predicted δ^{15}N can be directly compared to measured δ^{15}N in trapped air bubbles. In reality, a number of factors influence δ^{15}N in addition to gravitational enrichment, most notably thermal diffusion because of temperature gradients (Severinghaus et al., 1998) and

a convective zone at the top of the firn column because of strong surface winds and high porosity (Kawamura et al., 2006). These other factors are not generally known for past times. For these reasons the δ^{15}N calculated in this way should be viewed as a maximum estimate (at least for Antarctic sites, where thermal diffusion signals are small or negative).

As expected, the firn model is able to reproduce the observed Δages for Taylor Dome and Taylor Glacier with arbitrary accumulation rates (Figure 8). The necessary accumulation rates for Taylor Dome are extremely low during the LGM and of similar magnitude as in Morse et al. (2007). A different approach, using the glaciological thinning function to un-thin our new TD2015 age model, yields comparable results (dashed line in the figure). The fact that the modeled accumulation rate is lowest at 30 ka BP and not later is merely reflective of the fact that we use a steady state model that does not integrate accumulation over time, such that variations that are smaller than Δage should not be interpreted. The model does a good job of estimating δ^{15}N before and after the LGM, but it is unable to reproduce the measured δ^{15}N signal during the time of extremely low accumulation for Taylor Dome and also to a slightly lesser degree Taylor Glacier. The discrepancy could be explained by a substantial convective zone at the top of the firn column (as seen in one modern location with very low accumulation rates; Kawamura et al., 2013; Severinghaus et al., 2010) or it may be indicative of the fact that the model is ill-suited for such extreme conditions.

With an accumulation rate of <1 mm/year for several thousand years, hiatuses in the record are to be expected. But a long-term accumulation hiatus (several millennia) is unlikely because of the good agreement of Taylor Glacier and Taylor Dome nssCa records during the LGM (Figure 4). Shorter hiatuses on the order of up to 1,000 years are conceivable and possibly even likely in such a low accumulation setting.

4. Conclusions

We present new dust and temperature proxy records from a horizontal ice core on Taylor Glacier that are incompatible with synchronous North-South climate change in the Taylor Dome region and the North Atlantic as suggested by Steig et al. (1998). Following Mulvaney et al. (2000), we construct a new ice age time scale for Taylor Dome by synchronizing it with our well-dated Taylor Glacier record using the dust signal, supported by the argument that the close proximity of the Taylor Glacier and Taylor Dome deposition sites prohibits large differences in the dust records. For consistency, we also update the Taylor Dome gas time scale. The new TD2015 time scale covers 0 to 60 ka BP, and although it still suffers from poor resolution during the LGM and less than optimal data quality, it is a clear improvement on previous dating efforts. During the LGM, Taylor Dome experienced a period of extremely low accumulation, along with a Δage of 12,000 years, the underestimation of which led to the initial erroneous interpretation of a synchronous North-South warming. The Taylor Dome isotope record on the TD2015 chronology shows a similar deglacial transition as the rest of Antarctica. Nevertheless, an interesting and apparently unique feature of Taylor Dome, that most of the deglacial warming is complete by 14.7 ka BP (Steig et al., 2000) remains valid in our new chronology.

Our results highlight the difficulty of reconstructing Δage for low accumulation areas. Great care has to be taken when estimating accumulation rate histories and modelling Δage to transfer the (usually well-known) gas age time scale to the ice matrix. Ideally, the ice phase can be dated independently by, for example, tephra layers or dust synchronization. Applying the Δage history from another site, especially a high accumulation site as done, for example, in Fogwill et al. (2017), is unlikely to yield robust results.

The good quality of the dust data indicates that Taylor Glacier is valuable as a source of large volume samples for measurements of micro-particles and their isotopes in high temporal resolution for the section presented (49 to 16 ka BP) and most likely also for other time intervals (Aarons et al., 2017). More work is needed to establish precise ice age chronologies for the full deglaciation, or the penultimate interglacial, both of which have been identified and can be accessed at the glacier surface (Baggenstos et al., 2017).

The extremely low accumulation rate during the LGM has implications for our understanding of the hydrology and atmospheric circulation at that time. It is well known that accumulation can vary significantly on small spatial scales, for example, Morse et al. (1999) show a large gradient in accumulation across Taylor Dome at present. There is evidence that during the LGM this gradient was reversed, with moisture bearing storms arriving mainly from the North, whereas today they reach Taylor Dome from the South (Morse et al., 1998). This finding is strengthened by the higher reconstructed LGM accumulation rates for Taylor Glacier ice, which was deposited to the North of Taylor Dome. Another aspect to consider is wind scour from strong katabatic

winds with possible lee/luv effects around Taylor Dome. Whether this low accumulation anomaly was due to local topographical effects only or if it is part of a larger regional accumulation anomaly is still unclear. In this context, it should be noted that snow deposited on Taylor Dome during the LGM could have been blown away, carrying with it trace constituents such as ^{10}Be and dust. For this reason, a constant-flux assumption for these species (or equivalently, a spatially invariant flux to the ice) is unwarranted.

Acknowledgments
The US Antarctic Program provided outstanding logistical support. IDDO (Ice Drilling Design and Operations) provided the drilling systems. The Polar Geospatial Center (PGC) provided satellite imagery. We thank Paul Rose for being a whiz and keeping the chain saws running. Thomas Bauska, Christo Buizert, Michael Dyonisius, Xavier Fain, Benjamin Hmiel, Robb Kulin, James Lee, Chandra Llewellyn, Logan Mitchell, Avery Palardy, Hinrich Schaefer, and Adrian Schilt all helped with sampling in the field. We also thank students and staff of the DRI ice core lab, including Monica Arienzo, Nathan Chellman, and Larry Layman. The data and TD2015 age model are available for download as supporting information accompanying this publication or from the U.S. Antarctic Program Data Center (https://doi.org/10.15784/601103). Finally, we thank two anonymous reviewers for providing careful and constructive reviews.

References

Aarons, S. M., Aciego, S. M., Arendt, C. A., Blakowski, M. A., Steigmeyer, A., Gabrielli, P., et al. (2017). Dust composition changes from Taylor Glacier (East Antarctica) during the last glacial-interglacial transition: A multi-proxy approach. *Quaternary Science Reviews*, *162*, 60–71. https://doi.org/10.1016/j.quascirev.2017.03.011

Aarons, S., Aciego, S., Gabrielli, P., Delmonte, B., Koornneef, J., Wegner, A., & Blakowski, M. (2016). The impact of glacier retreat from the Ross Sea on local climate: Characterization of mineral dust in the Taylor Dome ice core, East Antarctica. *Earth and Planetary Science Letters*, *444*, 34–44. https://doi.org/10.1016/j.epsl.2016.03.035

Aciego, S. M., Cuffey, K. M., Kavanaugh, J. L., Morse, D. L., & Severinghaus, J. P. (2007). Pleistocene ice and paleo-strain rates at Taylor Glacier, Antarctica. *Quaternary Research*, *68*(3), 303–313. https://doi.org/10.1016/j.yqres.2007.07.013

Ahn, J., & Brook, E. J. (2007). Atmospheric CO_2 and climate from 65 to 30 ka B.P. *Geophysical Research Letters*, *34*, L10703. https://doi.org/10.1029/2007GL029551

Albani, S., Delmonte, B., Maggi, V., Baroni, C., Petit, J.-R., Stenni, B., et al. (2012). Interpreting last glacial to Holocene dust changes at Talos Dome (East Antarctica): Implications for atmospheric variations from regional to hemispheric scales. *Climate of the Past*, *8*(2), 741–750. https://doi.org/10.5194/cp-8-741-2012

Andersen, K. K., Svensson, A., Johnsen, S. J., Rasmussen, S. O., Bigler, M., Röthlisberger, R., et al. (2006). The Greenland Ice Core Chronology 2005, 15–42ka. Part 1: Constructing the time scale. *Quaternary Science Reviews*, *25*(23), 3246–3257. https://doi.org/10.1016/j.quascirev.2006.08.002

Armour, K. C., Marshall, J., Scott, J. R., Donohoe, A., & Newsom, E. R. (2016). Southern Ocean warming delayed by circumpolar upwelling and equatorward transport. *Nature Geoscience*, *9*, 549–554. https://doi.org/10.1038/ngeo2731

Baggenstos, D., Bauska, T. K., Severinghaus, J. P., Lee, J. E., Schaefer, H., Buizert, C., et al. (2017). Atmospheric gas records from Taylor Glacier, Antarctica, reveal ancient ice with ages spanning the entire last glacial cycle. *Climate of the Past*, *13*(7), 943–958. https://doi.org/10.5194/cp-13-943-2017

Basile, I., Grousset, F. E., Revel, M., Petit, J. R., Biscaye, P. E., & Barkov, N. I. (1997). Patagonian origin of glacial dust deposited in East Antarctica, (Vostok and Dome C) during glacial stages 2, 4 and 6. *Earth and Planetary Science Letters*, *146*(3–4), 573–589. https://doi.org/10.1016/S0012-821X(96)00255-5

Bauska, T. K., Baggenstos, D., Brook, E. J., Mix, A. C., Marcott, S. A., Petrenko, V. V., et al. (2016). Carbon isotopes characterize rapid changes in atmospheric carbon dioxide during the last deglaciation. *Proceedings of the National Academy of Sciences*, *113*(13), 3465–3470. https://doi.org/10.1073/pnas.1513868113

Bender, M. L., Floch, G., Chappellaz, J., Suwa, M., Barnola, J.-M., Blunier, T., et al. (2006). Gas age-ice age differences and the chronology of the Vostok ice core, 0-100 ka. *Journal of Geophysical Research*, *111*, D21115. https://doi.org/10.1029/2005JD006488

Bigler, M., Röthlisberger, R., Lambert, F., Stocker, T. F., & Wagenbach, D. (2006). Aerosol deposited in East Antarctica over the last glacial cycle: Detailed apportionment of continental and sea-salt contributions. *Journal of Geophysical Research*, *111*, D08205. https://doi.org/10.1029/2005JD006469

Blunier, T., Spahni, R., Barnola, J.-M., Chappellaz, J., Loulergue, L., & Schwander, J. (2007). Synchronization of ice core records via atmospheric gases. *Climate of the Past*, *3*(2), 325–330. https://doi.org/10.5194/cp-3-325-2007

Brook, E. J., Harder, S., Severinghaus, J., Steig, E. J., & Sucher, C. M. (2000). On the origin and timing of rapid changes in atmospheric methane during the last glacial period. *Global Biogeochemical Cycles*, *14*(2), 559–572. https://doi.org/10.1029/1999GB001182

Buiron, D., Chappellaz, J., Stenni, B., Frezzotti, M., Baumgartner, M., Capron, E., et al. (2011). Taldice-1 age scale of the Talos Dome deep ice core, East Antarctica. *Climate of the Past*, *7*(1), 1–16. https://doi.org/10.5194/cp-7-1-2011

Buiron, D., Stenni, B., Chappellaz, J., Landais, A., Baumgartner, M., Bonazza, M., et al. (2012). Regional imprints of millennial variability during the MIS 3 period around Antarctica. *Quaternary Science Reviews*, *48*, 99–112. https://doi.org/10.1016/j.quascirev.2012.05.023

Buizert, C., Cuffey, K. M., Severinghaus, J. P., Baggenstos, D., Fudge, T. J., Steig, E. J., et al. (2015). The WAIS Divide deep ice core WD2014 chronology - Part 1: Methane synchronization (68-31 ka BP) and the gas age-ice age difference. *Climate of the Past*, *11*(2), 153–173. https://doi.org/10.5194/cp-11-153-2015

Carlson, A. E., & Clark, P. U. (2012). Ice sheet sources of sea level rise and freshwater discharge during the last deglaciation. *Reviews of Geophysics*, *50*, RG4007. https://doi.org/10.1029/2011RG000371

Craig, H., Horibe, Y., & Sowers, T. (1988). Gravitational separation of gases and isotopes in polar ice caps. *Science*, *242*(4886), 1675–1678. https://doi.org/10.1126/science.242.4886.1675

Dansgaard, W. (1964). Stable isotopes in precipitation. *Tellus*, *16*(4), 436–468. https://doi.org/10.1111/j.2153-3490.1964.tb00181.x

Davis, P. T., Menounos, B., & Osborn, G. (2009). Holocene and latest Pleistocene alpine glacier fluctuations: a global perspective. *Quaternary Science Reviews*, *28*(21–22), 2021–2033. https://doi.org/10.1016/j.quascirev.2009.05.020

Delmonte, B., Baroni, C., Andersson, P. S., Schoberg, H., Hansson, M., Aciego, S., et al. (2010). Aeolian dust in the Talos Dome ice core (East Antarctica, Pacific/Ross Sea sector): Victoria Land versus remote sources over the last two climate cycles. *Journal of Quaternary Science*, *25*(8), 1327–1337. https://doi.org/10.1002/jqs.1418

Delmonte, B., Paleari, C. I., Andò, S., Garzanti, E., Andersson, P. S., Petit, J. R., et al. (2017). Causes of dust size variability in central East Antarctica (Dome B): Atmospheric transport from expanded South American sources during Marine Isotope Stage 2. *Quaternary Science Reviews*, *168*, 55–68. https://doi.org/10.1016/j.quascirev.2017.05.009

Delmonte, B., Petit, J. R., Andersen, K. K., Basile-Doelseh, I., Maggi, V., & Lipenkov, V. Y. (2004). Dust size evidence for opposite regional atmospheric circulation changes over east Antarctica during the last climatic transition. *Climate Dynamics*, *23*(3-4), 427–438. https://doi.org/10.1007/s00382-004-0450-9

Delmonte, B., Petit, J., & Maggi, V. (2002). Glacial to Holocene implications of the new 27000-year dust record from the EPICA Dome C (East Antarctica) ice core. *Climate Dynamics*, *18*(8), 647–660. https://doi.org/10.1007/s00382-001-0193-9

EPICA Community Members (2006). One-to-one coupling of glacial climate variability in Greenland and Antarctica. *Nature*, *444*(7116), 195–198. https://doi.org/10.1038/nature05301

Epstein, S., & Mayeda, T. (1953). Variation of O^{18} content of waters from natural sources. *Geochimica et Cosmochimica Acta*, *4*(5), 213–224. https://doi.org/10.1016/0016-7037(53)90051-9

Farmer, E. C., deMenocal, P. B., & Marchitto, T. M. (2005). Holocene and deglacial ocean temperature variability in the Benguela upwelling region: Implications for low-latitude atmospheric circulation. *Paleoceanography*, *20*, PA2018. https://doi.org/10.1029/2004PA001049

Fischer, H., Fundel, F., Ruth, U., Twarloh, B., Wegner, A., Udisti, R., et al. (2007). Reconstruction of millennial changes in dust emission, transport and regional sea ice coverage using the deep EPICA ice cores from the Atlantic and Indian Ocean sector of Antarctica. *Earth and Planetary Science Letters*, *260*(1–2), 340–354. https://doi.org/10.1016/j.epsl.2007.06.014

Fogwill, C. J., Turney, C. S. M., Golledge, N. R., Etheridge, D. M., Rubino, M., Thornton, D. P., et al. (2017). Antarctic ice sheet discharge driven by atmosphere-ocean feedbacks at the last glacial termination. *Scientific Reports*, *7*, 1–10. https://doi.org/10.1038/srep39979

Fudge, T. J., Waddington, E. D., Conway, H., Lundin, J. M. D., & Taylor, K. (2014). Interpolation methods for Antarctic ice-core timescales: application to Byrd, Siple Dome and Law Dome ice cores. *Climate of the Past*, *10*(3), 1195–1209. https://doi.org/10.5194/cp-10-1195-2014

Gooseff, M. N., Lyons, W. B., McKnight, D. M., Vaughn, B. H., Fountain, A. G., & Dowling, C. (2006). A stable isotopic investigation of a polar desert hydrologic system, McMurdo Dry Valleys, Antarctica. *Arctic Antarctic and Alpine Research*, *38*(1), 60–71. https://doi.org/10.1657/1523-0430(2006)038[0060:ASIIOA]2.0.CO;2

Goujon, C., Barnola, J.-M., & Ritz, C. (2003). Modeling the densification of polar firn including heat diffusion: Application to close-off characteristics and gas isotopic fractionation for Antarctica and Greenland sites. *Journal of Geophysical Research*, *108*(D24), 4792. https://doi.org/10.1029/2002JD003319

Grootes, P. M., Steig, E. J., Stuiver, M., Waddington, E. D., & Morse, D. L. (2001). The Taylor Dome Antarctic O-18 record and globally synchronous changes in climate. *Quaternary Research*, *56*(3), 289–298. https://doi.org/10.1006/qres.2001.2276

Grousset, F. E., Biscaye, P. E., Revel, M., Petit, J.-R., Pye, K., Joussaume, S., & Jouzel, J. (1992). Antarctic (Dome C) ice-core dust at 18 k.y. B.P.: Isotopic constraints on origins. *Earth and Planetary Science Letters*, *111*(1), 175–182. https://doi.org/10.1016/0012-821X(92)90177-W

Herron, M., & Langway, C. C. (1980). Firn densification: An empirical model. *Journal of Glaciology*, *25*, 373–385. https://doi.org/10.3189/S0022143000015239

Hoshina, Y., Fujita, K., Nakazawa, F., Iizuka, Y., Miyake, T., Hirabayashi, M., et al. (2014). Effect of accumulation rate on water stable isotopes of near-surface snow in inland Antarctica. *Journal of Geophysical Research: Atmospheres*, *119*, 274–283. https://doi.org/10.1002/2013JD020771

Indermühle, A., Monnin, E., Stauffer, B., Stocker, T. F., & Wahlen, M. (2000). Atmospheric CO_2 concentration from 60 to 20 kyr BP from the Taylor Dome Ice Core, Antarctica. *Geophysical Research Letters*, *27*(5), 735–738. https://doi.org/10.1029/1999GL010960

Indermühle, A., Stocker, T. F., Joos, F., Fischer, H., Smith, H. J., Wahlen, M., et al. (1999). Holocene carbon-cycle dynamics based on CO_2 trapped in ice at Taylor Dome, Antarctica. *Nature*, *398*(6723), 121–126. https://doi.org/10.1038/18158

Jouzel, J., Alley, R., Cuffey, K., Dansgaard, W., Grootes, P., Hoffmann, G., et al. (1997). Validity of the temperature reconstruction from water isotopes in ice cores. *Journal of Geophysical Research*, *102*(C12), 26,471–26,487. https://doi.org/10.1029/97JC01283

Jouzel, J., Masson, V., Cattani, O., Falourd, S., Stievenard, M., Stenni, B., et al. (2001). A new 27 ky high resolution East Antarctic climate record. *Geophysical Research Letters*, *28*(16), 3199–3202. https://doi.org/10.1029/2000GL012243

Kageyama, M., Merkel, U., Otto-Bliesner, B., Prange, M., Abe-Ouchi, A., Lohmann, G., et al. (2013). Climatic impacts of fresh water hosing under Last Glacial Maximum conditions: a multi-model study. *Climate of the Past*, *9*(2), 935–953. https://doi.org/10.5194/cp-9-935-2013

Kavanaugh, J. L., & Cuffey, K. M. (2009). Dynamics and mass balance of Taylor Glacier, Antarctica: 2. Force balance and longitudinal coupling. *Journal Of Geophysical Research*, *114*, F04011. https://doi.org/10.1029/2009JF001329

Kawamura, K., Severinghaus, J. P., Albert, M. R., Courville, Z. R., Fahnestock, M. A., Scambos, T., et al. (2013). Kinetic fractionation of gases by deep air convection in polar firn. *Atmospheric Chemistry and Physics*, *13*(21), 11,141–11,155. https://doi.org/10.5194/acp-13-11141-2013

Kawamura, K., Severinghaus, J. P., Ishidoya, S., Sugawara, S., Hashida, G., Motoyama, H., et al. (2006). Convective mixing of air in firn at four polar sites. *Earth and Planetary Science Letters*, *244*(3–4), 672–682. https://doi.org/10.1016/j.epsl.2006.02.017

Koci, B. R., & Kuivinen, K. C. (1984). Instruments and methods: The Pico lightweight coring auger. *Journal of Glaciology*, *30*(105), 244–245. https://doi.org/10.1017/S0022143000006018

Lambert, F., Delmonte, B., Petit, J. R., Bigler, M., Kaufmann, P. R., Hutterli, M. A., et al. (2008). Dust-climate couplings over the past 800,000 years from the EPICA Dome C ice core. *Nature*, *452*(7187), 616–619. https://doi.org/10.1038/nature06763

Landais, A., Barnola, J., Kawamura, K., Caillon, N., Delmotte, M., Ommen, T. V., et al. (2006). Firn-air $\delta^{15}N$ in modern polar sites and glacial-interglacial ice: A model-data mismatch during glacial periods in Antarctica? *Quaternary Science Reviews*, *25*(1–2), 49–62. https://doi.org/10.1016/j.quascirev.2005.06.007

Lisiecki, L. E., & Lisiecki, P. A. (2002). Application of dynamic programming to the correlation of paleoclimate records. *Paleoceanography*, *17*(4), 1049. https://doi.org/10.1029/2001PA000733

Lourantou, A., Lavrič, J. V., Köhler, P., Barnola, J.-M., Paillard, Michel, E., et al. (2010). Constraint of the CO_2 rise by new atmospheric carbon isotopic measurements during the last deglaciation. *Global Biogeochemical Cycles*, *24*, GB2015. https://doi.org/10.1029/2009GB003545

Lunt, D. J., & Valdes, P. J. (2001). Dust transport to Dome C, Antarctica, at the Last Glacial Maximum and present day. *Geophysical Research Letters*, *28*(2), 295–298. https://doi.org/10.1029/2000GL012170

Mahowald, N., Kohfeld, K., Hansson, M., Balkanski, Y., Harrison, S. P., Prentice, I. C., et al. (1999). Dust sources and deposition during the last glacial maximum and current climate: A comparison of model results with paleodata from ice cores and marine sediments. *Journal of Geophysical Research*, *104*(D13), 15,895–15,916. https://doi.org/10.1029/1999JD900084

Marcott, S. A., Bauska, T. K., Buizert, C., Steig, E. J., Rosen, J. L., Cuffey, K. M., et al. (2014). Centennial-scale changes in the global carbon cycle during the last deglaciation. *Nature*, *514*(7524), 616–619. https://doi.org/10.1038/nature13799

Maselli, O. J., Fritzsche, D., Layman, L., McConnell, J. R., & Meyer, H. (2013). Comparison of water isotope-ratio determinations using two cavity ring-down instruments and classical mass spectrometry in continuous ice-core analysis. *Isotopes in Environmental and Health Studies*, *49*(3), 387–398. https://doi.org/10.1080/10256016.2013.781598

Masson-Delmotte, V., Buiron, D., Ekaykin, A., Frezzotti, M., Gallée, H., Jouzel, J., et al. (2011). A comparison of the present and last interglacial periods in six Antarctic ice cores. *Climate of the Past*, *7*(2), 397–423. https://doi.org/10.5194/cp-7-397-2011

McConnell, J. R., Aristarain, A. J., Banta, J. R., Edwards, P. R., & Simões, J. C. (2007). 20th-century doubling in dust archived in an Antarctic Peninsula ice core parallels climate change and desertification in South America. *Proceedings of the National Academy of Sciences*, *104*(14), 5743–5748. https://doi.org/10.1073/pnas.0607657104

McConnell, J. R., Burke, A., Dunbar, N. W., Köhler, P., Thomas, J. L., Arienzo, M. M., et al. (2017). Synchronous volcanic eruptions and abrupt climate change ~17.7 ka plausibly linked by stratospheric ozone depletion. *Proceedings of the National Academy of Sciences*, *114*(38), 10,035–10,040. https://doi.org/10.1073/pnas.1705595114

McConnell, J. R., Lamorey, G. W., Lambert, S. W., & Taylor, K. C. (2002). Continuous ice-core chemical analyses using inductively coupled plasma mass spectrometry. *Environmental Science & Technology*, *36*(1), 7–11. https://doi.org/10.1021/es011088z

McManus, J. F., Francois, R., Gherardi, J. M., Keigwin, L. D., & Brown-Leger, S. (2004). Collapse and rapid resumption of Atlantic meridional circulation linked to deglacial climate changes. *Nature*, *428*(6985), 834–837. https://doi.org/10.1038/nature02494

Monnin, E., Steig, E. J., Siegenthaler, U., Kawamura, K., Schwander, J., Stauffer, B., et al. (2004). Evidence for substantial accumulation rate variability in Antarctica during the Holocene, through synchronization of CO_2 in the Taylor Dome, Dome C and DML ice cores. *Earth and Planetary Science Letters*, *224*(1–2), 45–54. https://doi.org/10.1016/j.epsl.2004.05.007

Morgan, V., Delmotte, M., van Ommen, T., Jouzel, J., Chappellaz, J., Woon, S., et al. (2002). Relative timing of deglacial climate events in Antarctica and Greenland. *Science*, *297*(5588), 1862–1864. https://doi.org/10.1126/science.1074257

Morse, D. L., Waddington, E. D., Marshall, H.-P., Neumann, T. A., Steig, E. J., Dibb, J. E., et al. (1999). Accumulation rate measurements at Taylor Dome, East Antarctica: Techniques and strategies for mass balance measurements in polar environments. *Geografiska Annaler: Series A, Physical Geography*, *81*(4), 683–694. https://doi.org/10.1111/1468-0459.00106

Morse, D. L., Waddington, E. D., & Rasmussen, L. A. (2007). Ice deformation in the vicinity of the ice-core site at Taylor Dome, Antarctica, and a derived accumulation rate history. *Journal of Glaciology*, *53*(182), 449–460. https://doi.org/10.3189/002214307783258530

Morse, D. L., Waddington, E. D., & Steig, E. J. (1998). Ice age storm trajectories inferred from radar stratigraphy at Taylor Dome, Antarctica. *Geophysical Research Letters*, *25*(17), 3383–3386. https://doi.org/10.1029/98GL52486

Mulvaney, R., Röthlisberger, R., Wolff, E. W., Sommer, S., Schwander, J., Hutteli, M. A., & Jouzel, J. (2000). The transition from the last glacial period in inland and near-coastal Antarctica. *Geophysical Research Letters*, *27*(17), 2673–2676. https://doi.org/10.1029/1999GL011254

Neumann, T., Waddington, E., Steig, E., & Grootes, P. (2005). Non-climate influences on stable isotopes at Taylor Mouth, Antarctica. *Journal of Glaciology*, *51*(173), 248–258. https://doi.org/10.3189/172756505781829331

Pedro, J. B., van Ommen, T. D., Rasmussen, S. O., Morgan, V. I., Chappellaz, J., Moy, A. D., et al. (2011). The last deglaciation: Timing the bipolar seesaw. *Climate of the Past*, *7*(2), 671–683. https://doi.org/10.5194/cp-7-671-2011

Petrenko, V. V., Smith, A. M., Brook, E. J., Lowe, D., Riedel, K., Brailsford, G., et al. (2009). $^{14}CH_4$ measurements in Greenland ice: Investigating Last Glacial Termination CH_4 sources. *Science*, *324*(5926), 506–508. https://doi.org/10.1126/science.1168909

Rasmussen, S. O., Andersen, K. K., Svensson, A. M., Steffensen, J. P., Vinther, B. M., Clausen, H. B., et al. (2006). A new Greenland ice core chronology for the last glacial termination. *Journal of Geophysical Research*, *111*, D06102. https://doi.org/10.1029/2005JD006079

Reeh, N., Oerter, H., Letréguilly, A., Miller, H., & Hubberten, H.-W. (1991). A new, detailed ice-age oxygen-18 record from the ice-sheet margin in central West Greenland. *Global and Planetary Change*, *4*(4), 373–383. https://doi.org/10.1016/0921-8181(91)90003-F

Ruth, U., Barbante, C., Bigler, M., Delmonte, B., Fischer, H., Gabrielli, P., et al. (2008). Proxies and measurement techniques for mineral dust in Antarctic ice cores. *Environmental Science & Technology*, *42*(15), 5675–5681. https://doi.org/10.1021/es703078z

Schoenemann, S. W., Steig, E. J., Ding, Q., Markle, B. R., & Schauer, A. J. (2014). Triple water-isotopologue record from WAIS Divide, Antarctica: Controls on glacial-interglacial changes in $^{17}O_{excess}$ of precipitation. *Journal of Geophysical Research: Atmospheres*, *119*, 8741–8763. https://doi.org/10.1002/2014JD021770

Schüpbach, S., Federer, U., Kaufmann, P. R., Albani, S., Barbante, C., Stocker, T. F., & Fischer, H. (2013). High-resolution mineral dust and sea ice proxy records from the Talos Dome ice core. *Climate of the Past*, *9*(6), 2789–2807. https://doi.org/10.5194/cp-9-2789-2013

Schwander, J., Sowers, T., Barnola, J.-M., Blunier, T., Fuchs, A., & Malaizé, B. (1997). Age scale of the air in the summit ice: Implication for glacial-interglacial temperature change. *Journal of Geophysical Research*, *102*(D16), 19,483–19,493. https://doi.org/10.1029/97JD01309

Schwander, J., Stauffer, B., & Sigg, A. (1988). Air mixing in firn and the age of the air at pore close-off. *Annals of Glaciology*, *10*, 141–145. https://doi.org/10.1017/S0260305500004328

Seltzer, A. M., Buizert, C., Baggenstos, D., Brook, E. J., Ahn, J., Yang, J.-W., & Severinghaus, J. P. (2017). Does $\delta^{18}O$ of O_2 record meridional shifts in tropical rainfall? *Climate of the Past*, *13*(10), 1323–1338. https://doi.org/10.5194/cp-13-1323-2017

Severinghaus, J. P., Albert, M. R., Courville, Z. R., Fahnestock, M. A., Kawamura, K., Montzka, S. A., et al. (2010). Deep air convection in the firn at a zero-accumulation site, central Antarctica. *Earth and Planetary Science Letters*, *293*(3-4), 359–367. https://doi.org/10.1016/j.epsl.2010.03.003

Severinghaus, J. P., Sowers, T., Brook, E. J., Alley, R. B., & Bender, M. L. (1998). Timing of abrupt climate change at the end of the Younger Dryas interval from thermally fractionated gases in polar ice. *Nature*, *391*(6663), 141–146. https://doi.org/10.1038/34346

Siddall, M., Milne, G. A., & Masson-Delmotte, V. (2012). Uncertainties in elevation changes and their impact on Antarctic temperature records since the end of the last glacial period. *Earth and Planetary Science Letters*, *315-316*, 12–23. https://doi.org/10.1016/j.epsl.2011.04.032

Sigl, M., Fudge, T. J., Winstrup, M., Cole-Dai, J., Ferris, D., McConnell, J. R., et al. (2016). The WAIS Divide deep ice core WD2014 chronology – Part 2: Annual-layer counting (0–31BP). *Climate of the Past*, *12*(3), 769–786. https://doi.org/10.5194/cp-12-769-2016

Sigl, M., McConnell, J. R., Toohey, M., Curran, M., Das, S. B., Edwards, R., et al. (2014). Insights from Antarctica on volcanic forcing during the Common Era. *Nature Climate Change*, *4*, 693–697. https://doi.org/10.1038/nclimate2293

Simonsen, M. F., Cremonesi, L., Baccolo, G., Bosch, S., Delmonte, B., Erhardt, T., et al. (2018). Particle shape accounts for instrumental discrepancy in ice core dust size distributions. *Climate of the Past*, *14*(5), 601–608. https://doi.org/10.5194/cp-14-601-2018

Smith, H. J., Fischer, H., Wahlen, M., Mastroianni, D., & Deck, B. (1999). Dual modes of the carbon cycle since the Last Glacial Maximum. *Nature*, *400*(6741), 248–250. https://doi.org/10.1038/22291

Sowers, T., Bender, M., & Raynaud, D. (1989). Elemental and isotopic composition of occluded O_2 and N_2 in polar ice. *Journal of Geophysical Research*, *94*(D4), 5137–5150. https://doi.org/10.1029/JD094iD04p05137

Steig, E. J., Brook, E. J., White, J. W. C., Sucher, C. M., Bender, M. L., Lehman, S. J., et al. (1998). Synchronous climate changes in Antarctica and the North Atlantic. *Science*, *282*(5386), 92–95. https://doi.org/10.1126/science.282.5386.92

Steig, E. J., Morse, D. L., Waddington, E. D., Stuiver, M., Grootes, P. M., Mayewski, P. A., et al. (2000). Wisconsinan and Holocene climate history from an ice core at Taylor Dome, western Ross Embayment, Antarctica. *Geografiska Annaler Series A Physical Geography*, *82*(2–3), 213–235. https://doi.org/10.1111/j.0435-3676.2000.00122.x

Steig, E. J., Polissar, P. J., Stuiver, M., Grootes, P. M., & Finkel, R. C. (1996). Large amplitude solar modulation cycles of Be-10 in Antarctica: Implications for atmospheric mixing processes and interpretation of the ice core record. *Geophysical Research Letters*, *23*(5), 523–526. https://doi.org/10.1029/96GL00255

Stenni, B., Buiron, D., Frezzotti, M., Albani, S., Barbante, C., Bard, E., et al. (2011). Expression of the bipolar see-saw in Antarctic climate records during the last deglaciation. *Nature Geoscience*, *4*(1), 46–49. https://doi.org/10.1038/ngeo1026

Stocker, T. F., & Johnsen, S. J. (2003). A minimum thermodynamic model for the bipolar seesaw. *Paleoceanography*, *18*(4), 1087. https://doi.org/10.1029/2003PA000920

Sucher, C. M. (1997). Atmospheric gases in the Taylor Dome ice core: Implications for East Antarctic climate change (Master's thesis), University of Rhode Island, Narragansett.

Timmermann, A., Menviel, L., Okumura, Y., Schilla, A., Merkel, U., Timm, O., et al. (2010). Towards a quantitative understanding of millennial-scale Antarctic warming events. *Quaternary Science Reviews*, *29*(1-2), 74–85. https://doi.org/10.1016/j.quascirev.2009.06.021

Toggweiler, J., & Samuels, B. (1995). Effect of Drake Passage on the global thermohaline circulation. *Deep Sea Research Part I: Oceanographic Research Papers*, *42*(4), 477–500. https://doi.org/10.1016/0967-0637(95)00012-U

Veres, D., Bazin, L., Landais, A., Toyé Mahamadou Kele, H., Lemieux-Dudon, B., Parrenin, F., et al. (2013). The Antarctic ice core chronology (AICC2012): an optimized multi-parameter and multi-site dating approach for the last 120 thousand years. *Climate of the Past*, *9*(4), 1733–1748. https://doi.org/10.5194/cp-9-1733-2013

WAIS Divide Project Members (2013). Onset of deglacial warming in West Antarctica driven by local orbital forcing. *Nature*, *500*(7463), 440–444. https://doi.org/10.1038/nature12376

WAIS Divide Project Members (2015). Precise interpolar phasing of abrupt climate change during the last ice age. *Nature*, *520*(7549), 661–665. https://doi.org/10.1038/nature14401

Waddington, E., Steig, E., & Neumann, T. (2002). Using characteristic times to assess whether stable isotopes in polar snow can be reversibly deposited. *Annals of Glaciology*, *35*, 118–124. https://doi.org/10.3189/172756402781817004

Wegner, A. (2008). Sources and transport characteristics of mineral dust in Dronning Maud Land Antarctica (PhD Thesis), Universität Bremen.

Wolff, E. W., Fischer, H., Fundel, F., Ruth, U., Twarloh, B., Littot, G. C., et al. (2006). Southern Ocean sea-ice extent, productivity and iron flux over the past eight glacial cycles. *Nature*, *440*(7083), 491–496. https://doi.org/10.1038/nature04614